Benchmarking High-Resolution, Hydrologic Model Performance of Long-Term Retrospectives in the Contiguous United States

Erin Towler[1], Sydney S. Foks[2], Aubrey L. Dugger[1], Jesse E. Dickinson[3], Hedeff I. Essaid[4], David Gochis[1], Roland J. Viger[2], and Yongxin Zhang[1]

[1]National Center for Atmospheric Research (NCAR), Boulder, CO, USA
[2]U.S. Geological Survey (USGS), Lakewood, CO, USA
[3]U.S. Geological Survey, Arizona Water Science Center, Tucson, AZ, USA
[4]U.S. Geological Survey, Moffett Field, CA, USA

Correspondence to: Erin Towler (towler@ucar.edu)

Abstract. Because use of high-resolution hydrologic models is becoming more widespread and estimates are made over large domains, there is a pressing need for systematic evaluation of their performance. Most evaluation efforts to date focus on smaller basins that have been relatively undisturbed by human activity, but there is also a need to benchmark model performance more comprehensively, including basins impacted by human activities. This study benchmarks the long-term performance of two process-oriented, high-resolution, continental-scale hydrologic models that have been developed to assess water availability and risks in the United States (US): the National Water Model v2.1 application of WRF-Hydro (NWMv2.1) and the National Hydrologic Model v1.0 application of the Precipitation-Runoff Modeling System (NHMv1.0). The evaluation is performed on 5,390 streamflow gages from 1983 to 2016 (~33 years) at a daily time step, including both natural and human-impacted catchments, representing one of the most comprehensive evaluations over the contiguous US. Using the Kling-Gupta efficiency as the main evaluation metric, the models are compared against a climatological benchmark that accounts for seasonality. Overall, the model applications show similar performance, with better performance in minimally disturbed basins than in those impacted by human activities. Relative regional differences are also similar: best performance is found in the Northeast, followed by the Southeast, and generally worse performance in the Central and West. For both models, about 80 percent of the sites exceed the seasonal climatological benchmark. Basins that do not exceed the climatological benchmark are further scrutinized to provide model diagnostics for each application. Using the underperforming subset, both models tend to overestimate streamflow volumes in the West, which could be attributed to not accounting for human activities, such as active management. Both models underestimate flow variability, especially the highest flows; this was more pronounced for the NHMv1.0. Low flows tended to be overestimated by the NWMv2.1, whereas for the NHMv1.0 there were both over and underestimations, but they were less severe. Although this study focused on model diagnostics for underperforming sites based on the seasonal climatological benchmark, metrics for all sites for both model applications are openly available online.

1 Introduction

Across the hydrologic modelling community, there is a pressing need for more systematic documentation and evaluation of continental-scale land surface and streamflow model performance (Famiglietti et al., 2011). A challenge to hydrologic evaluation stems from the fact that the objectives of hydrologic modelling often vary. Archfield et al. (2015) reviewed how different communities have approached hydrologic modelling in the past, drawing a distinction between hydrologic catchment modelers whose primary interest has been simulating streamflow at the local to regional scale, versus land surface modelers, who have historically focused on the water cycle as it relates to atmospheric and evaporative processes at the global scale. As modelling approaches have advanced toward coupled hydrologic and atmospheric systems, both perspectives have evolved and are converging towards the goal of improving hydrologic model performance through more intentional evaluation and benchmarking efforts.

Land surface modelling (LSM) has a rich history of community-developed benchmarking and intercomparison projects (van den Hurk et al., 2011; Best et al., 2015). In addition to comparative evaluations of process-based models, the LSM community has used statistical benchmarks, which in some cases have been shown to make better use of the forcing input data than state-of-the-art LSMs (Abramowitz et al., 2008; Nearing et al., 2018). The International Land Model Benchmarking (ILAMB) project is an international benchmarking framework developed by the LSM community (Luo et al., 2012) and has been applied to comprehensively evaluate Earth system models, including the categories of biogeochemistry, hydrology, radiation and energy, and climate forcing (Collier et al., 2018). Although hydrology is a component of ILAMB and other LSM benchmarking efforts, there is a need for closer collaboration with hydrologists to improve hydrologic process representation in these models (Clark et al., 2015).

Hydrologic catchment modelling has begun to move towards large-sample hydrology, an extension of comparative hydrology, where model performance is evaluated for a large sample of catchments, rather than focusing solely on individual watersheds. This is appealing since evaluating hydrologic models across a wide variety of hydrologic regimes facilitates more robust regional generalizations and comparisons (Gupta et al., 2014). As such, many hydrologic modelling evaluation efforts have begun to encompass larger spatial scales. Monthly water balance models have been used to relate contiguous US (CONUS) model errors to hydroclimatic variables (Martinez and Gupta, 2010) and for parameter regionalization (Bock et al., 2016). As part of the North American Land Data Assimilation System project phase 2, Xia et al. (2012) evaluate simulated streamflow for four land surface models, focusing mostly on 961 small basins, as well as eight major river basins in the CONUS, finding that the ensemble mean performs better than the individual models. Further, several large-sample datasets have been developed for community use. The Model Parameter Estimation Experiment (MOPEX) includes hydrometeorological time series and land surface attributes for hydrological basins in the US and globally that have minimal human impacts (Duan et al. 2006). The more recent Catchment Attributes and Meteorology for Large-sample Studies (CAMELS) dataset includes

hydrometeorological data and catchment attributes for 600+ small- to medium-sized basins in the CONUS (Addor et al. 2017).

65   By using CAMELS basins that are minimally disturbed by human activities, Newman et al. (2015, 2017) and Addor et al. (2018) are able to attribute regional variations in model performance to continental-scale factors. Knoben et al. (2020) also use CAMELS with 36 lumped conceptual models, finding that model performance is more strongly linked to streamflow signatures than to climate or catchment characteristics.

70   While these efforts are useful towards evaluating smaller, minimally impacted basins, there is also a need to benchmark model performance for larger basins, including those impacted by human activities. On the global scale, catchment techniques have been applied to global hydrologic modelling, and have been shown to outperform traditional gridded global models of river flow (Arheimer et al. 2020). On the regional scale, Lane et al. (2019) benchmark the predictive capability of river flow for over 1,000 catchments in Great Britain by using four lumped hydrological models; Lane et al. (2019) include both natural and

75   human-impacted catchments, finding poor performance when the water budget is not closed, such as due to non-modelled human impacts. Mai et al. (2022) conducted a systematic intercomparison study over the Great Lakes Region, finding that regionally calibrated models suffer from poor performance in urban, managed, and agricultural areas. Tijerina et al. (2021) compared performance of two high-resolution models that incorporate lateral subsurface flow at 2,200 streamflow gages; they found poor performance in the central US, potentially due to non-modelled groundwater abstraction and irrigation, during a

80   one-year study period. As hydrologic model development moves to include human systems, these studies provide important baselines.

This study builds on previous large-sample studies by benchmarking long-term retrospective streamflow simulations over the CONUS. Specifically, two high-resolution, process-oriented models are evaluated that have been developed to address water

85   issues nationally: the National Water Model v2.1 application of WRF-Hydro (NWMv2.1; Gochis et al., 2020a) and the National Hydrologic Model v1.0 application of the Precipitation-Runoff Modeling System (NHMv1.0; Regan et al., 2018). The evaluation is performed on daily streamflow for 5,390 streamflow gages from 1983-2016 (~33 years), including both natural and human-impacted catchments, representing one of the most comprehensive evaluations over the CONUS to date. The model performance is compared against a climatological benchmark that accounts for seasonality, and results are examined

90   in terms of spatial patterns and human influences. The climatological seasonal benchmark is used as a threshold to screen the sites for each model application, offering a way to target the results for model diagnostics and development.

2 Hydrologic Model Descriptions

2.1 The National Water Model v2.1 application of WRF-Hydro (NWMv2.1)

The National Center for Atmospheric Research (NCAR) has developed an open-source, spatially distributed, physics-based

95   community hydrologic model, WRF-Hydro (Gochis et al. 2020a; Gochis et al. 2020b), which is the current basis for the

National Oceanic and Atmospheric Administration's National Water Model (NWM). The NWM is an operational hydrologic modeling system simulating and forecasting major water components (e.g., evapotranspiration, snow, soil moisture, groundwater, surface inundation, reservoirs, streamflow) in real-time across the CONUS, Hawaii, Puerto Rico, and the US Virgin Islands. NWM streamflow simulations from version 2.1 CONUS long-term retrospective analysis (NWMv2.1) are used. The retrospective data are available from public cloud data outlets (e.g., compressed netcdf files can be found at: https://noaa-nwm-retrospective-2-1-pds.s3.amazonaws.com/index.html). More information on these data is available from the Office of Water Prediction (OWP) National Water Model (OWP, 2022) and release notes (Farrar 2019).

NWMv2.1 is forced by 1-km atmospheric states and fluxes from NOAA's Analysis of Record for Calibration (AORC; National Weather Service, 2021). For the land surface model, NWMv2.1 uses the Noah-MP (Noah-multiparameterization; Niu et al., 2011), which calculates energy and water states and vertical fluxes on a 1-km grid. WRF-Hydro physics-based hydrologic routing schemes transport surface water and shallow saturated soil water laterally across a 250-m resolution terrain grid and into channels. NWMv2.1 also leverages WRF-Hydro's conceptual baseflow parameterization, which approximates deeper groundwater storage and release through a simple exponential decay model. The three-parameter Muskingum–Cunge river routing scheme is used to route streamflow on an adapted National Hydrography Dataset Plus (NHDPlus) version 2 (McKay et al., 2012) river network representation (Gochis et al., 2020a). A level-pool scheme is activated on 5,783 lakes and reservoirs across CONUS representing passive storage and releases from waterbodies; however, no active reservoir management is currently included in the NWM. While the operational NWM does include data assimilation, there is no data assimilation applied in the retrospective simulation used here. Using the AORC meteorological forcings, NWMv2.1 calibrates a subset of 14 soil, vegetation, and baseflow parameters to streamflow in 1,378 gauged, predominantly natural flow basins. The calibration procedure uses the Dynamically Dimensioned Search algorithm (Tolson and Shoemaker, 2007) to optimize parameters to a weighted Nash-Sutcliffe efficiency (NSE; Nash and Sutcliffe 1970) of hourly streamflow (mean of the standard NSE and log-transformed NSE). Calibration runs separately for each calibration basin, then a hydrologic similarity strategy is used to regionalize parameters to the remaining basins within the model domain. The calibration period was from water years 2008 – 2013, and 2014-2016 water years were used for validation. For the retrospective analysis, NWMv2.1 produces the channel network output (streamflow, velocity), reservoir output (inflow, level, outflow) and groundwater output (inflow, level, outflow) every hour and every 3 hours for land model output (e.g., snow, evapotranspiration, soil moisture) and high-resolution terrain output (shallow water table depth, ponded water depth). For this analysis, hourly streamflow is aggregated to daily averages.

2.2 The National Hydrologic Model v1.0 application of the Precipitation-Runoff Modelling System (NHMv1.0)

The U.S. Geological Survey (USGS) has developed the National Hydrologic Model (NHM version 1.0) application of the Precipitation-Runoff Modelling System (PRMS) (Regan et al., 2018). PRMS uses a deterministic, physical-process representation of water flow and storage between the atmosphere and land surface, including snowpack, canopy, soil, surface depression, groundwater storage, and stream networks. Used here are the NHM daily discharge simulations from version v1.0

(NHMv1.0) and more specifically, results from the calibration workflow "by headwater calibration using observed streamflow" with the Muskingum-Mann streamflow routing option ("byHRU_musk_obs"; Hay and LaFontaine, 2020).

Climate inputs to the NHMv1.0 are 1-km resolution daily precipitation and daily maximum and minimum temperature from Daymet (version 3; Thornton et al., 2018). The geospatial structure, which defines the default parameters, spatial hydrologic response units (HRUs) and the stream network, is defined by the geospatial fabric version 1.0 (Viger and Bock, 2014). The NHM is calibrated using a multiple-objective, stepwise approach to identify an optimal parameter set that balances water budgets and streamflow. The first step calibrates for the water balance of each spatial HRU to "baseline" observations of runoff, actual evapotranspiration, soil moisture, recharge, and snow-covered area derived from multiple datasets (Hay and LaFontaine, 2020). The second step considers timing of streamflow by calibration to statistically generated streamflow in 7,265 headwater watersheds having drainage area of less than 3,000 km^2. The final step calibrates to observed gaged streamflow at 1,417 streamgage locations; details of the calibration can be seen in Appendix 1 of LaFontaine et al. (2019). The calibration period included the odd water years from 1981-2010, and the even water years from 1982-2010 were used for validation. The NHM does not simulate reservoir operations, surface or groundwater withdrawals, or stream releases. The NHM outputs daily streamflow, which is used in the analysis here.

3 Evaluation Approach

3.1 Data

This study evaluates daily simulations from October 1, 1983 to December 31, 2016, or just over 33 years (=~12,100 days). Model simulations are compared to observations at 5,390 USGS stations (Foks et al., 2022); stations were included that had a minimum data length of at least 8 years or 2,920 daily observations (i.e., ~25% complete data), though the observations did not need to be continuous (this allows for missing data, including intermittent and/or seasonally operated gages). A subset of these gages (n = 5,389) also occurs in the Geospatial Attributes of Gages for Evaluating Streamflow, version II dataset (GAGES II; Falcone, 2011), therefore attributes from GAGES-II are used to examine select results. Figure 1 shows the spatial distribution of the gages, along with their designated region; regions are further aggregations of Level II ecoregions as defined by GAGES-II (see Figure 1 caption). Figure 1 shows the uneven distribution of gages: the eastern United States has a dense network of gages, followed by decreasing coverage moving west into the central plains. There is a modest increase in gage density across the intermountain west, and higher coverage along the west coast. Figure 1 also shows the classification, that is, if the site has been characterized as Reference or Non-Reference. Reference gages indicate less-disturbed watersheds, and observations associated with Non-Reference gages have some level of anthropogenic influence (Falcone 2011). Although the Non-Reference gages outnumber the Reference gages by about 4 to 1, Reference gages are relatively well-distributed through the regions.

3.2 Metrics

Table 1 shows the metrics used in the evaluation, as well as their descriptions. Metrics were calculated in the statistical software R (R Core Team, 2021), including using the hydroGOF (hydrological goodness of fit) package (Zambrano-Bigiarini, 2020).

The Kling-Gupta efficiency (KGE) is used as the overall performance metric, which is defined as (Gupta et al. 2009):

$$KGE = 1 - \sqrt{(r-1)^2 + \left(\frac{\sigma_{sim}}{\sigma_{obs}} - 1\right)^2 + \left(\frac{\mu_{sim}}{\mu_{obs}}\right)^2}$$

where r is the linear (Pearson) correlation coefficient between the observations (obs) and simulations (sim), σ is the standard deviation of the flows, and μ is the mean. The KGE components of r and the ratio of standard deviations between the simulations and observed (rSD) are also examined. Correlation quantifies the relationship between modelled and observed streamflow and is often used to assess flow timing. The rSD shows the relative variability (Gupta et al., 2009; Newman et al., 2017), indicating if the model is over- or underestimating the variability of the simulated state (in this case, daily streamflow), relative to observations. In this evaluation, instead of using the ratio of means component, the related percent bias (PBIAS) is calculated (Zambrano-Bigiarini 2020):

$$PBIAS = \frac{\sum_{t=1}^{N}(S_t - O_t)}{\sum_{t=1}^{N} O_t}$$

where observed flow is O, simulated flow is S, and t = 1, 2,… N is the time series flow index. Percent bias (PBIAS) provides information on if the model is over- or underestimating the total streamflow volume (based on the entire simulation period).

To provide context for the interpretation of the KGE scores, a lower benchmark must be specified (Pappenberger et al., 2015; Schaefli and Gupta, 2007; Seibert, 2001; Seibert et al., 2018). The KGE does not include a built-in lower benchmark in its formulation, but Knoben et al. (2019) show that models with KGE scores higher than −0.41 contribute more information than the mean flow benchmark. Recently, Knoben et al. (2020) show that it is more robust to define a lower benchmark that considers seasonality. Hence, a reference time series based on the average and median flows for each day-of-year is used to calculate a lower KGE value which serves as a climatological (lower) benchmark.

Two additional hydrologic signatures are included which evaluate performance based on different parts of the flow duration curve (FDC) for high and low flows. The definitions of these hydrologic signatures are consistent with those from Yilmaz et al. (2008). The bias of high flows (the top 2%) is computed to evaluate how well the model captures the watershed response to big precipitation or melt events (PBIAS_HF). For low flows, the bias of the bottom 30% (PBIAS_LF), offers insight into baseflow performance. Equations for these two metrics can be found in the online Supplemental Material.

190 Using daily observations and model simulations, the evaluation metrics from Table 1 are calculated for each of the gages for the NWMv2.1 (Towler et al., 2022a) and NHMv1.0 (Towler et al., 2022b) hydrologic modelling applications. As mentioned, to produce a seasonal climatological benchmark, KGE is also calculated using daily observations and day-of-year averages and medians for each site; these KGE scores are referred to as AvgDOY and MedDOY, respectively.

4 Results

195

KGE scores for the benchmarks and models are presented as a cumulative density functions (CDFs; Figure 2), and Table 2 quantifies the percent of sites less than or greater than select KGE scores. First, the seasonal benchmarks and model KGE scores can be compared to the mean flow benchmark (i.e., KGE <-0.41; Knoben et al. 2019): for the MedDOY, 18% of sites have lower scores (Table 2). Zero percent of sites have lower scores than the KGE benchmark if the AvgDOY is used instead of the median flow (i.e., 0% in Table 2). For the models, at 14% of the sites the NWMv2.1 simulations do not provide more

200 skill than the mean flow benchmark, similar to 12% of sites using NHMv1.0. The CDFs for the models intersect with the AvgDOY curve at a KGE score of about -0.06; at this value, 19%-20% of the sites perform worse in terms of KGE using the model simulation, whereas above this value the model simulations perform better than AvgDOY. In terms of median values, the AvgDOY (MedDOY) has a median KGE of 0.08 (-0.1), while the NWMv2.1 has a median of 0.53 and the NHMv1.0

205 median is 0.46. Given the better performance of AvgDOY in comparison to MedDOY, only AvgDOY is used as the lower benchmark in the forthcoming analyses.

KGE performance is also examined by whether it has been classified as Reference or Non-Reference. Figure 3 shows KGE scores as CDFs for the models and the AvgDOY benchmark broken out by this classification. As expected, the AvgDOY

210 curves are virtually identical regardless of classification. However, for both models, the Reference gages are outperforming the Non-Reference gages. Table 3 shows the median values for the models: for the NHMv1.0, the KGE is 0.67 (0.38) for the Reference (Non-Reference), and for NWMv2.1 it is 0.65 for the Reference versus 0.49 for the Non-Reference. Looking at the components, the r values are the same for both model Reference sites (0.78). For the PBIAS, the NHMv1.0 shows underestimation for both Reference and Non-Reference sites (-4.1% and -5.7%, respectively), but the NWMv2.1

215 underestimates (-4.0%) at the Reference sites and overestimates (5.3%) at the Non-Reference sites.

Figure 4 shows KGE scores as CDFs for the models broken out by region. The model applications are similar, but there are notable differences by region. In general, performance is best for the Northeast, followed by the Southeast. Central and West perform the worst, although West exhibits some high KGE values. Table 4 shows the median KGE, r, rSD, and PBIAS values

220 broken out by region, showing the biggest differences in PBIAS among regions and between models. Regional variability can be further examined by the KGE maps for the models: in the West, more of the poor performing sites are in the arid Southwest

and the lower elevation basins in the intermountain West; better performance is seen in the higher elevations in the intermountain West and West Coast, including the Pacific Northwest (Figure 5A for NWMv2.1 and Figure 5B for NHMv1.0). Figure 5 shows that for both models in the Central region, relatively poor performance is concentrated along the plains areas that span from the high plains (i.e., North Dakota) vertically down through the center of the CONUS (i.e., South Dakota, Nebraska, Kansas, Texas). Performance is more mixed as one moves further east in the Central region (e.g., around the Great Lakes). Relatively uniform good performance is seen in the Southeast. However, as previously mentioned, the model results need to be placed into context by comparing with a climatological benchmark. Figure 6 shows the KGE map for the AvgDOY, which has relatively higher KGE values mostly in parts of the western CONUS, where there are notable seasonal signatures (e.g., snowmelt runoff), and relatively lower KGE values in most of the other regions. By taking KGE differences by site, it is easier to examine where the model applications are doing relatively better and worse than the seasonal benchmark. Figure 7 shows the spatial distribution of the KGE differences, where the model with the maximum KGE value is used (i.e., maximum between the $KGE_{NWMv2.1}$ and $KGE_{NHMv1.0}$). Overall, the model applications tend to outperform the AvgDOY benchmark, except in the West & western Central regions. Supplemental Figure 1 shows that if the AvgDOY benchmark is outperformed, it is usually by both models (at 63% of sites); this is similar to the findings of Knoben et al. (2020). KGE difference maps for each individual model follow the same general spatial pattern (Supplemental Figures 2 and 3).

Basins that do not exceed the climatological benchmark are further scrutinized for each model application to offer insights towards model diagnostics and development; that is, only sites that have KGE scores worse than the AvgDOY benchmark are examined from here forward. From here forward, these are called "underperforming sites". By classification, most underperforming sites are human impacted (90-93%, see Table 5). By region, most underperforming sites are in the West (55-67%) or Central (23-28%) regions (Table 6). Next, the bias metrics can be examined to try to determine why these sites are not able to beat the climatological benchmark. Spatial maps of PBIAS shows that the NWMv2.1 (Figure 8A) generally overestimates volume; NHMv1.0 (Figure 8B) is more mixed with underestimation in the Central region. Both models overestimate water volumes in the West. This could be because neither model is capturing active reservoir operations or water extractions (e.g., for irrigation), which is important since water is heavily managed in the West. This is different than the overall distribution of PBIAS for the modelling applications, where if you look at all the gages (n=5,390), PBIAS for both models is centered around zero (Supplemental Figure 4). The underestimation in the Central region for the NHMv1.0, which is absent in NWMv2.1, could be due to the different time steps of the models, where NWMv2.1 is run hourly and NHMv1.0 is run daily; this hypothesis is expanded upon in the Discussion section. Maps for PBIAS_HF can be seen in Supplemental Figure 5; for PBIAS_HF, the overall distribution of PBIAS_HFs is centered below zero, indicating that the models tend to underestimate high flows, but for the underperforming gages this is more pronounced in the NHMv1.0 than then NWMv2.1 (Supplemental Figure 6). Results for rSD paint a similar picture: both models tend to underestimate variability, but the underestimation is more pronounced in NHMv1.0 (Supplemental Figures 7 and 8). Figure 9 shows PBIAS_LF for both model

255 applications: the NWMv2.1 tends to overestimate the low flows, whereas the NHMv1.0 is more mixed and the over- or underestimation is less severe. This can also be seen in the histograms for PBIAS_LF (Supplemental Figure 9).

5 Discussion and Conclusions

Water availability is a critical concern worldwide, and its assessment extends beyond the individual catchment scale, needing to include basins large and small, influenced by human activities and not. As such, large-sample hydrologic modeling and
260 evaluation has taken on a new urgency, especially as these models are used to assess water availability and risks. In the US, the high-resolution model applications benchmarked here are two widely used federal hydrologic models, providing information at spatial and temporal scales that are vital to realizing water security. To our knowledge, this is the first time that these models have been evaluated so comprehensively, as this analysis included daily simulations at 5,390 gages, over a 33-year period, and includes basins both impacted and non-impacted by human activities. Further, a climatological seasonal
265 benchmark is used to provide an a priori expectation of what constitutes as a "good" model. This analysis is aligned with recent aims of the hydrologic benchmarking community to put performance metrics in context (Clark et al. 2021; Knoben et al. 2020). This paper extends this approach by demonstrating how the climatological benchmark can be used as a threshold to further scrutinize errors at underperforming sites. This is complementary to other model diagnostic and development work that aims to understand model sensitivity and why models improve/degrade with changes. Recent studies have applied sensitivity
270 analyses that consider both parametric and structural uncertainties to identify the water cycle components streamflow predictions are most sensitive to (Mai et al., 2022). Information theory also provides tools that help identify model components contributing to errors (Frame et al. 2021). Further, simple statistical or conceptual models (e.g., Nearing et al., 2018; Newman et al., 2017) could also be used as a benchmark if applied to the same sites/catchments and time periods.

275 In terms of KGE, the model applications showed similar performance, despite differences in process representations, parameter estimation strategies, meteorological forcings, and space/time discretizations. Reference gages performed better than the Non-Reference gages, and regionally the best performance was seen in the Northeast, followed by the Southeast, with worse performance in the Central and West, although the West has some high KGE scores. Further, for both models, most of the sites were able to beat the seasonal benchmark, and the majority of sites that did not were Non-Reference. Despite different forcings
280 (NWMv2.1 is forced by AORC and NHMv1.0 is forced by Daymet version 3), the model applications had generally similar performance. Although outside the scope of this study, further exploration of streamflow biases due to forcing biases could offer insights on error sources. Further, the calibration periods of the models differed, and both overlapped with the evaluation period used in this study. While this overlap can introduce biases into the evaluation process, it allowed us to evaluate long-term performance for the same sites and time periods for both models. While this is not without precedent (e.g., Duan et al.
285 2006), recent studies are exploring best practices for calibration and validation to improve model robustness and generalizability (Shen et al. 2022).

PBIAS results showed that for both models, simulated streamflow volumes are overestimated in the West region, particularly for the sites designated as Non-Reference. One likely reason for this is that water withdrawal for human use is endemic throughout the West and neither model has a thorough representation of these withdrawals. Furthermore, neither model possesses significant representations for lake and stream channel evaporation which, through the largely semi-arid West, can constitute a significant amount of water "loss" to the hydrologic system (Friedrich et al., 2018). Lastly, nearly all western rivers are also subject to some form of impoundment. Even neglecting evaporative, seepage and withdrawal losses from these water bodies, the storage and timed releases of water from managed reservoirs can significantly alter flow regimes from daily to seasonal timescales thereby degrading model performance statistics at gaged locations downstream of those reservoirs. Lane et al. (2019) find that poor model performance occurs when the water budget is not closed, such as when human modifications or groundwater processes are not accounted for in the models. As model development moves towards including human systems, the benchmark results provide a concrete goal for "how much" improvement could be necessary to be achieved by a management module. This addition of management could support decision makers as they grapple with how to account for the anthropogenic influence on watersheds, especially since most studies to date focus on minimally disturbed sites.

Another interesting difference in PBIAS was seen in the Central US, where the NHMv1.0 is underestimating volumes at underperforming sites. As detailed in the model descriptions, the model applications are run at different temporal scales: NHMv1.0 is run daily, whereas NWMv2.1 is run hourly and aggregated to daily. One hypothesis is that some precipitation events that are occurring on sub-daily scales, like convective storms and the associated runoff modes (Buchanan et al. 2018) may be missed. Similarly, while both models tend to underestimate high flows (PBIAS_HF) and variability (rSD), this is more pronounced for the NHMv1.0, which is in line with this hypothesis. The model applications showed differences in PBIAS_LF, with the NWMv2.1 overestimating low flows, whereas while the NHMv1.0 both over- and underestimated them it was less severe. Both models used in the applications benchmarked here have only rudimentary representation of groundwater processes. Additional attributes (e.g., baseflow or aridity indices) could be strategically identified to further understand these model errors and differences. Model target applications, which drive model developer selections for process representation, space and time discretization, and calibration objectives, also have a notable imprint on the performance. The NWMv2.1, with a focus on flood prediction and fast (hourly) timescales, shows better performance in high-flow-focused metrics, while the NHMv1.0, designed for water availability assessment and slower (daily) timescales, shows more balanced and better performance in low-flow-focused metrics.

Identifying a suite of evaluation metrics has an element of subjectivity, but our aim was to focus on streamflow magnitude, since these model applications were developed to inform water availability assessments. However, magnitude is only one aspect of streamflow, and different metrics for other categories (e.g., frequency, duration, and rate of change) could be more appropriate for addressing specific scientific questions or modeling objectives. Recently, McMillan (2019) links hydrologic

signatures to specific processes using only streamflow and precipitation. McMillan (2019) does not find many signatures that relate to human alteration; however, in this paper, the streamflow bias metrics are found to be useful in this regard. One limitation of this study is that it does not consider the sensitivity of the KGE to sampling uncertainty, which can be large for heavy-tailed streamflow errors (Clark et al., 2021). This could be addressed by applying bootstrapping methods (Clark et al., 2021). Alternative estimators of KGE that are more appropriate for skewed streamflow data (e.g., LBE from Lamontagne et al., 2020) could be added in the future, but currently require separate treatment of sites with zero streamflow, which was not feasible for this initial evaluation. Finally, some of the metrics in the benchmark suite include redundant error information; one approach to remedy this has been put forth by Hodson et al. (2021), where the mean log square error is decomposed to only include independent error components (see Hodson et al. 2021 for details). This could also be addressed using Empirical Orthogonal Function (EOF) analysis, which has been done for climate model evaluation (Rupp et al., 2013).

In closing, this paper uses the climatological seasonal benchmark as a threshold to screen sites for each model application. While this fit with the purpose of this study, the metrics for NWMv2.1 (Towler et al. 2022a) and NHMv1.0 (Towler et al. 2022b) are available for all sites (Foks et al. 2022); these can be analyzed and/or screened as needed. In the future, it could also be useful to extend the analysis beyond streamflow to other water budget components to assess additional aspects of model performance.

Code and data availability:

NWMv2.1 model data can be accessed through an Amazon S3 bucket, https://registry.opendata.aws/nwm-archive/, and NHMv1.0 model data are available as a USGS data release (Hay and Fontaine 2020).   Metrics results discussed in this publication can be found in Towler et al. (2022a, 2022b).

Author Contributions:

ET and SSF collaborated to develop and demonstrate the evaluation and study design; ALD, JED, HIE, DG, and RJV contributed to discussions that shaped the ideas. ET led the results analysis and prepared the original paper and revisions. All authors helped with the editing and revisions of the paper. YZ ran the NWM model and provided the data.

Competing interests: The authors declare that they have no conflict of interest.

Acknowledgements: We thank the USGS HyTEST Evaluation task team (Robert W. Dudley, Krista A. Dunne, Glenn A. Hodgkins, Timothy O. Hodson, Sara B. Levin, Thomas M. Over, Colin A Penn, Amy M. Russell, Samuel W. Saxe, Caelan E. Simeone) for feedback on the development of the evaluation and study design and the WRF-Hydro group (in particular Ryan Cabell, Andy Gaydos, Alyssa McCluskey, Arezoo Rafieeinasab, Kevin Sampson, and Tim Schneider). We thank Stacey

355 Archfield and Andrew Newman for comments on an earlier version of the manuscript. We thank Robert Chlumsky and two anonymous referees for reviewing the paper. Any use of trade, firm, or product names is for descriptive purposes only and does not imply endorsement by the U.S. Government.

Financial Support: This research was supported by the U.S. Geological Survey (USGS) Water Mission Area's Integrated Water
360 Prediction Program. National Center for Atmospheric Research (NCAR) is a major facility sponsored by the National Science Foundation (NSF) under Cooperative Agreement 1852977.

References

Abramowitz, G., Leuning, R., Clark, M., and Pitman A.J.: Evaluating the performance of land surface models, J. Climate, 21, 5468–5481, 2008.

365

Addor, N., Nearing, G., Prieto, C.,Newman, A. J., Le Vine, N., and Clark, M. P.: A ranking of hydrological signatures based on their predictability in space, Water Resour. Res., 54, 8792–8812, https://doi.org/10.1029/2018WR022606, 2018.

Addor, N., Newman, A. J., Mizukami, N., and Clark, M. P.: The CAMELS data set: catchment attributes and meteorology for
370 large-sample studies, Hydrol. Earth Syst. Sci., 21, 5293–5313, https://doi.org/10.5194/hess-21-5293-2017, 2017.

Archfield, S. A., Clark, M., Arheimer, B., Hay, L. E., Mcmillan, H., Kiang, J. E., … Farmer, W. H.: Accelerating advances in continental domain hydrologic modeling, Water Resour. Res., 10078–10091, https://doi.org/10.1002/2015WR017498, 2015.

375 Arheimer, B., Pimentel, R., Isberg, K., Crochemore, L., Andersson, J.C.M., Hasan, A., and Pineda, L.: Global catchment modelling using World-Wide HYPE (WWH),open data, and stepwise parameter estimation, Hydrol. Earth Syst. Sci., 24, 535–559, https://doi.org/10.5194/hess-24-535-2020, 2020.

Best, M. J., and Coauthors: The plumbing of land surface models: Benchmarking model performance, J. Hydrometeor., 16,
380 1425–1442, doi:10.1175/JHM-D-14-0158.1, 2015.

Bock, A.R., Hay, L.E., McCabe, G.J., Markstrom, S.L., and Atkinson, R.D.: Parameter regionalization of a monthly water balance model for the conterminous United States, Hydrol. Earth Syst. Sci., 20, 2861–2876, https://doi.org/10.5194/hess-20-2861-2016., 2016.

385

Buchanan, B., Auerbach, D.A., Knighton, J., Evensen, D., Fuka, D.R., Easton, Z. Wieczorek, M., Archibald, J.A., McWilliams, B., and Walter, T.: Estimating dominant runoff modes across the conterminous United States, Hydrological Processes, 32: 3881–3890, https://doi.org/10.1002/hyp.13296, 2018.

390   Clark, M. P., Fan, Y., Lawrence, D.M., Adam, J.C., Bolster, D., Gochis D.J., Hooper, R.P., Kumar, M., Leung L.R., …, and Zeng X.: Improving the representation of hydrologic processes in Earth System Models, Water Resour. Res., 51, 5929–5956, doi:10.1002/2015WR017096, 2015.

Clark, M. P., Vogel, R. M., Lamontagne, J. R., Mizukami, N., Knoben, W. J. M., Tang, G., et al.: The abuse of popular
395   performance metrics in hydrologic modeling, Water Resour. Res., 57, e2020WR029001. https://doi.org/10.1029/2020WR029001, 2021.

Collier, N., Hoffman, F. M., Lawrence, D. M., Keppel-Aleks, G., Koven, C. D., Riley, W. J., … Randerson, J. T.: The International Land Model Benchmarking (ILAMB) System: Design, Theory, and Implementation, Journal of Advances in
400   Modeling Earth Systems, 10(11), 2731–2754, https://doi.org/10.1029/2018MS001354, 2018.

Duan, Q., Schaake, J., Andréassian, V., Franks, S., Goteti, G., Gupta, H. V., et al. (2006). Model parameter estimation experiment (MOPEX): An overview of science strategy and major results from the second and third workshops. Journal of Hydrology, 320(1–2), 3–17. https://doi.org/10.1016/j.jhydrol.2005.07.031

405
ESRI: USA States Generalized Boundaries [Data set], ESRI, https://esri.maps.arcgis.com/home/item.html?id=8c2d6d7df8fa4142b0a1211c8dd66903, 2022a.

ESRI: World Countries (Generalized) [Data set], ESRI, https://hub.arcgis.com/datasets/esri::world-countries-
410   generalized/about, 2022b.

Falcone, J. A.: *GAGES-II: Geospatial attributes of gages for evaluating streamflow*. US Geological Survey, 2011.

Famiglietti, J.S., Murdoch, L., Lakshmi, V., Arrigo, J., and Hooper, R.: Establishing a Framework for Community Modeling
415   in Hydrologic Science, 3rd Workshop on Community Hydrologic Modeling Platform (CHyMP), available at: https://www.cuahsi.org/uploads/library/CUAHSI-TR10.pdf (last access March 10, 2022), 2011.

Farrar, M.: Service Change Notice, https://www.weather.gov/media/notification/pdf2/scn20-119nwm_v2_1aad.pdf, Access Date: Nov 9, 2022; 2021.

420   Foks, S.S., Towler, E., Hodson, T.O., Bock, A.R., Dickinson, J.E., Dugger, A.L., Dunne, K.A., Essaid, H.I., Miles, K.A., Over, T.M., Penn, C.A., Russell, A.M., Saxe, S.W., and Simeone, C.E.: Streamflow benchmark locations for conterminous United States, version 1.0 (cobalt gages): U.S. Geological Survey data release, https://doi.org/10.5066/P972P42Z, 2022.

425   Frame, J.M., Kratzert, F., Raney II, A., Rahman, M., Salas F.R., and Nearing G.S.: Post-Processing the National Water Model with Long Short-Term Memory Networks for Streamflow Predictions and Model Diagnostics, JAWRA, https://doi.org/10.1111/1752-1688.12964, 2021.

Friedrich, K., Grossman, R.L., Huntington, J., Blanken, P.D., Lenters, J., Holman, K.D., Gochis, D., Livneh, B., Prairie, J., 430   Skeie, E., Healey, N.C., Dahm, K., Pearson, C., Finnessey, T., Hook, S.J., Kowalski, T.: Reservoir evaporation in the Western United States, Bull. Am. Meteorol. Soc., https://doi.org/10.1175/BAMS-D-15-00224.1, 2018.

Gochis, D.J., Barlage, M., Cabell, R., Casali, M., Dugger, A., FitzGerald, K., McAllister, M., McCreight, J., RafieeiNasab, A., Read, L., Sampson, K., Yates, D., and Zhang Y: The WRF-Hydro® modeling system technical description, (Version 5.1.1). 435   NCAR Technical Note. 107 pages. Available online at: https://ral.ucar.edu/sites/default/files/public/projects/wrf-hydro/technical-description-user-guide/wrf-hydrov5.2technicaldescription.pdf, 2020a.

Gochis, D., Barlage, M., Cabell, R., Dugger, A., Fanfarillo, A., FitzGerald, K., McAllister, M., McCreight, J., RafieeiNasab, A., Read, L., Frazier, N., Johnson, D., Mattern, J. D., Karsten, L., Mills, T. J., and Fersch, B.: WRF-Hydro v5.1.1, Zenodo 440   [data set], https://doi.org/10.5281/zenodo.3625238, 2020b.

Grannemann, N. G.: Great Lakes and Watersheds Shapefiles [Data set], USGS, https://www.sciencebase.gov/catalog/item/530f8a0ee4b0e7e46bd300dd, 2010.

Gupta, H. V, Kling, H., Yilmaz, K. K., and Martinez, G. F.: Decomposition of the mean squared error and NSE performance criteria: Implications for improving hydrological modelling, *Journal of Hydrology*, *377*(1–2), 80–91, 445   https://doi.org/10.1016/j.jhydrol.2009.08.003, 2009.

Gupta, H.V., Perrin, C., Blöschl, G, Montanari, A., Kumar, R., Clark, M., and Andréassian, V.: Large-sample hydrology: a need to balance depth with breadth, Hydrol. Earth Syst. Sci., 18, 463–477, https://doi.org/10.5194/hess-18-463-2014, 2014.

Hay, L.E., and LaFontaine, J.H.: Application of the National Hydrologic Model Infrastructure with the Precipitation-Runoff Modeling System (NHM-PRMS),1980-2016, Daymet Version 3 calibration: U.S. Geological Survey data release, https://doi.org/10.5066/P9PGZE0S, 2020.

Hodson, T.O., Over, T.M., and Foks, S.F.: Mean squared error, deconstructed, Journal of Advances in Modeling Earth Systems, https://doi.org/10.1029/2021MS002681, 2021.

Knoben, W.J.M., Freer, J.E., and Woods, R.: (2019). Technical note: Inherent benchmark or not? Comparing Nash-Sutcliffe and Kling-Gupta efficiency scores. Hydrology and Earth System Sciences Discussions. 1-7. 10.5194/hess-2019-327.

Knoben, W.J.M., Freer, J.E., Peel, M. C., Fowler, K. J. A., &Woods, R. A. (2020). A brief analysisof conceptual model structureuncertainty using 36 models and 559catchments.Water Resources Research,56, e2019WR025975. https://doi.org/10.1029/2019WR025975

LaFontaine, J. H., Hart, R. M., Hay, L. E., Farmer, W. H., Bock, A. R., Viger, R. J., Markstrom, S.L., Regan, R.S., Driscoll, J. M.: Simulation of water availability in the Southeastern United States for historical and potential future climate and land-cover conditions, U.S. Geological Survey Scientific Investigations Report 2019–5039, 83 p., https://doi.org/10.3133/sir20195039, 2019.

Lamontagne, J. R., Barber C., and Vogel R.M.: Improved estimators of model performance efficiency for skewed hydrologic data, Water Resour. Res., 56 (9), e2020WR027101, https://doi.org/10.1029/2020WR027101, 2020.

Lane, R. A., Coxon, G., Freer, J. E., Wagener, T., Johnes, P. J., Bloomfield, J. P., … Reaney, S. M.: Benchmarking the predictive capability of hydrological models for river flow and flood peak predictions across over 1000 catchments in Great Britain. Hydrol. Earth Syst. Sci., 23(10), 4011–4032. https://doi.org/10.5194/hess-23-4011-2019, 2019.

Luo, Y. Q., Randerson, J. T., Abramowitz, G., Bacour, C., and Al., E.: A framework for benchmarking land models, Biogeosciences, 3857–3874. https://doi.org/10.5194/bg-9-3857-2012, 2012.

Mai, J., Craig, J.R., Tolson, B.A., and Arsenault, R.: The sensitivity of simulated streamflow to individual hydrologic processes across North America, Nature Communications, 13(455), https://doi.org/10.1038/s41467-022-28010, 2022.

Mai, J., Shen, H., Tolson, B. A., Gaborit, É., Arsenault, R., Craig, J. R., Fortin, V., Fry, L. M., Gauch, M., Klotz, D., Kratzert, F., O'Brien, N., Princz, D. G., Rasiya Koya, S., Roy, T., Seglenieks, F., Shrestha, N. K., Temgoua, A. G. T., Vionnet, V., and

Waddell, J. W.: The Great Lakes Runoff Intercomparison Project Phase 4: The Great Lakes (GRIP-GL) Hydrol. Earth Syst. Sci., 26, 3537–3572, 2022.

Martinez, G.F., and Gupta, H.V.: Toward improved identification of hydrological models: A diagnostic evaluation of the "abcd" monthly water balance model for the conterminous United States, Water Resour. Res., 46, W08507, doi:10.1029/2009WR008294, 2010.

McKay, L., Bondelid, T., Dewald, T., Johnston, J., Moore, R., and Rea, A.: NHDPlus Version 2: user guide, National Operational Hydrologic Remote Sensing Center, Washington, DC, 2012.

McMillan, H: Linking hydrologic signatures to hydrologic processes: A review, Hydrological Processes, 34: 1393–1409, https://doi.org/10.1002/hyp.13632, 2019.

Nash, J. E. and Sutcliffe, J. V.: River flow forecasting through conceptual models. Part I: A discussion of principles, J. Hydrol., 10, 282–290, doi:10.1016/0022-1694(70)90255-6, 1970.

National Weather Service: Analysis of Record for Calibration: Version 1.1 Sources, Methods, and Verification. Retrieved from: https://hydrology.nws.noaa.gov/aorc-historic/Documents/AORC-Version1.1-SourcesMethodsandVerifications.pdf (last access March 17, 2022), 2021.

Natural Earth Data: Ocean (version 5.1.1) [Data set], Natural Earth Data, https://www.naturalearthdata.com/downloads/10m-physical-vectors/10m-ocean/, 2009.

Nearing, G. S., Ruddell, B. L., Clark, M. P., Nijssen, B., and Peters-Lidard, C.: Benchmarking and process diagnostics of land models, *Journal of Hydrometeorology*, *19*(11), 1835–1852. https://doi.org/10.1175/JHM-D-17-0209.1, 2018.

Newman, A. J., Clark, M. P., Sampson, K., Wood, A., Hay, L. E., Bock, A., … and Duan, Q.: Development of a large-sample watershed-scale hydrometeorological data set for the contiguous USA: Data set characteristics and assessment of regional variability in hydrologic model performance, Hydrol. Earth Syst. Sci., *19*(1), 209–223. https://doi.org/10.5194/hess-19-209-2015, 2015.

Newman, A. J., Mizukami, N., Clark, M. P., Wood, A. W., Nijssen, B., and Nearing, G.: Benchmarking of a physically based hydrologic model, Journal of Hydrometeorology, 18, 2215–2225. https://doi.org/10.1175/JHM-D-16-0284.1, 2017.

Niu, G.-Y., Yang, Z.-L., Mitchell, K. E., Chen, F., Ek, M. B., Barlage, M., Kumar, A., Manning, K., Niyogi, D., Rosero, E., Tewari, M., and Xia, Y.: The community Noah land surface model with multiparameterization options (Noah-MP): 1. Model

description and evaluation with local-scale measurements, J. Geophys. Res., 116, D12109, https://doi.org/10.1029/2010JD015139, 2011.

Office of Water Prediction (OWP): The National Water Model, https://water.noaa.gov/about/nwm, Access date: Nov 9, 2022.

Pappenberger, F., Ramos, M. H., Cloke, H. L., Wetterhall, F., Alfieri, L., Bogner, K., et al.: How do I know if my forecasts are better? Using benchmarks in hydrological ensemble prediction, Journal of Hydrology, 522, 697–713, https://doi.org/10.1016/j.jhydrol.2015.01.024, 2015.

R Core Team: R: A language and environment for statistical computing. R Foundation for Statistical Computing, Vienna, Austria, available at: https://www.r-project.org (last access: 4 May 2022), 2021.

Regan et al (2018) Description of the National Hydrologic Model for use with the PRMS, USGS Techniques and Methods, 6-B9, https://doi.org/10.3133/tm6B9

Rupp, D.E., Abatzoglou, J.T., Hegewisch, K.C., and Mote, P.W.: Evaluation of CMIP5 20th century climate simulations for the Pacific Northwest USA, Journal of Geophysical Research: Atmospheres, https://doi.org/10.1002/jgrd.50843, 2013.

Schaefli, B., and Gupta, H.V.: Do Nash values have value? Hydrol. Process. 21 (15), 2075–2080, 2007.

Seibert, J.: On the need for benchmarks in hydrological modelling, Hydrological Processes, 15(6), 1063–1064, 2001.

Seibert, J., Vis, M. J. P., Lewis, E., and van Meerveld, H. J.: (2018). Upper and lower benchmarks in hydrological modelling.HydrologicalProcesses,32(8), 1120–1125, https://doi.org/10.1002/hyp.11476, 2018.

Shen, H., Tolson, B. A., & Mai, J. (2022). Time to update the split-sample approach in hydrological model calibration. Water Resources Research, 58, e2021WR031523.

Tijerina, D., Condon, L., FitzGerald, K., Dugger, A., O'Neill, M. M., Sampson, K., … Maxwell, R.: Continental Hydrologic Intercomparison Project, Phase 1: A large-scale hydrologic model comparison over the continental United States, Water Resour. Res., 57(7), 1–27. https://doi.org/10.1029/2020wr028931, 2021.

Tolson, B.A., and Shoemaker C.A., Dynamically Dimensioned Search Algorithm for Computationally Efficient Watershed Model Calibration, Water Resour. Res., DOI:10.1029/2005WR004723, 2007.

550 Towler, E., Foks, S.S., Dickinson, J.E., Dugger, A.L., Essaid, H.I., Gochis, D., Hodson, T.O., Viger, R.J., and Zhang Y.: Daily streamflow performance benchmark defined by the standard statistical suite (v1.0) for the National Water Model Retrospective (v2.1) at benchmark streamflow locations: U.S. Geological Survey data release, https://doi.org//10.5066/P9QT1KV7, 2022a.

Towler, E., Foks, S.S., Dugger, A.L., Dickinson, J.E., Essaid, H.I., Hodson, T.O., and Viger, R.J.: Daily streamflow performance benchmark defined by the standard statistical suite (v1.0) for the National Hydrologic Model application of the Precipitation-Runoff Modeling System (v1 byObs Muskingum) at benchmark streamflow locations: U.S. Geological Survey 555 data release, https://doi.org/10.5066/P9DKA9KQ , 2022b.

Thornton, P.E., Thornton, M.M., Mayer, B.W., Wei, Y., Devarakonda, R., Vose, R.S., Cook, R.B.: Daymet: Daily Surface Weather Data on a 1-km Grid for North America, Version 3. ORNL DAAC, Oak Ridge, Tennessee, USA, at https://doi.org/10.3334/ORNLDAAC/1328, 2017.

560 van den Hurk, B., M. Best, P. Dirmeyer, A. Pitman, J. Polcher, and Santanello, J.: Acceleration of land surface model development over a decade of GLASS, Bull. Am. Meteorol. Soc., 92, 1593–1600, 2011.

Viger, R.J., and Bock, A.: GIS features of the geospatial fabric for national hydrologic modeling: U.S. Geological Survey data release, http://dx.doi.org/doi:10.5066/ F7542KMD, 2014.

565

Yilmaz, K., Gupta, H., and Wagener, T.: A process-based diagnostic approach to model evaluation: Application to the NWS distributed hydrologic model, *Water Resour. Res., 44*, 2008.

Zambrano-Bigiarini M.: Package 'hydroGOF', available online at: https://github.com/hzambran/hydroGOF (last access April 570 12, 2022), 2020.

Tables

 Table 1. Evaluation metrics calculated on the daily streamflows. KGE = Kling–Gupta efficiency; rSD = ratio of standard deviations between simulations and observed; PBIAS = percent bias; HF = high flows; LF = low flows; Inf= infinity; USGS = United States Geological Survey; ft3/s = cubic feet per second.

Statistic	Description	Range (Perfect)	Comments
KGE	Kling–Gupta efficiency (Gupta et al., 2009)	-Inf to 1 (1)	Normalized hydrologic metric of overall performance geared towards high flows (sensitive to outliers); calculated from KGE in R package hydroGOF.
r	Pearson's correlation coefficient	-1 to 1 (1)	Pearson (linear estimator) of correlation; calculated from rPearson in R Package hydroGOF.
rSD	Ratio of standard deviations	0 to Inf (1)	Indicates if flow variability is being over- or underestimated; calculated from rSD in R Package hydroGOF.
PBIAS	Percent bias	-100 to Inf (0)	Indicates if total streamflow volume is being over- or underestimated; calculated from pbias in R Package hydroGOF.
PBIAS_HF	Percent bias of flows >=Q98 (Yilmaz et al. 2008)	-100 to Inf (0)	Characterizes response to large precipitation events; calculated using flows >= the 98th percentile flow using pbias in R Package hydroGOF.
PBIAS_LF	Percent bias of flows <=Q30 (Yilmaz et al. 2008)	-Inf to 100 (0)	Characterizes baseflow; calculated following equations in Yilmaz et al. (2008) using logged flows <= the 30th percentile (zeros are set to USGS observational threshold of 0.01 ft3/s).

 Table 2. Median Kling-Gupta efficiency (KGE) scores and percent of sites (p) less than or greater than given KGE scores for seasonal benchmarks based on the median day-of-year flows (MedDOY) and average day-of-year flows (AvgDOY), and the models: National Water Model v2.1 (NWMv2.1) and National Hydrologic Model v1.0 (NHMv1.0).

KGE Source	KGE Median	p(KGE<-0.41)	p(KGE<-0.06)	p(KGE>0.50)	p(KGE>0.75)
MedDOY	-0.13	18%	59%	5.7%	0.2%
AvgDOY	0.08	0%	19%	8.4%	1.5%
NHMv1.0	0.46	12%	20%	46%	15%
NWMv2.1	0.53	14%	19%	54%	16%

 Table 3. Median values broken out by Reference (Ref, n= 1,115) and Non-Reference (Non-ref, n= 4,274) gages (one gage was not designated as Ref or Non-ref and is therefore not included). KGE = Kling–Gupta efficiency; r = Pearson's corelation coefficient, rSD = ratio of standard deviations between simulations and observed; PBIAS = percent bias; NHMv1.0=National Hydrologic Model v1.0; NWMv2.1 = National Water Model v2.1.

Model	Class	KGE	r	rSD	PBIAS
NHMv1.0	Non-ref	0.38	0.72	0.86	-5.7
	Ref	0.67	0.78	0.84	-4.1
NWMv2.1	Non-ref	0.49	0.75	0.92	5.3
	Ref	0.65	0.78	0.87	-4.0

Table 4. Median values for each region. KGE = Kling–Gupta efficiency; r = Pearson's correlation coefficient, rSD = ratio of standard deviations between simulations and observed; PBIAS = percent bias; NHMv1.0=National Hydrologic Model v1.0; NWMv2.1 = National Water Model v2.1.

Region	Model	KGE	r	rSD	PBIAS
West	NHMv1.0	0.29	0.74	0.98	9.3
	NWMv2.1	0.32	0.75	1.17	27
Central	NHMv1.0	0.33	0.68	0.78	-18
	NWMv2.1	0.45	0.71	0.87	4.4
Southeast	NHMv1.0	0.48	0.73	0.78	-11
	NWMv2.1	0.56	0.77	0.85	-1.1
Northeast	NHMv1.0	0.63	0.78	0.86	-3.0
	NWMv2.1	0.65	0.79	0.82	-7.8

595

Table 5. The number (percent) of sites in each classification for each hydrologic model application where the KGE score is less than the average day-of-year flow (AvgDOY) benchmark (underperforming sites); KGE = Kling–Gupta efficiency; NHMv1.0=National Hydrologic Model v1.0; NWMv2.1 = National Water Model v2.1; max(Model) = model with maximum KGE value from NHMv1.0 or NWMv2.1; Ref = Reference (minimal human impacts); Non-Ref = Non-Reference (influenced by human activities).

600

Model	Class	n (%)
NHMv1.0	Ref	137 (9.4%)
	Non-Ref	1319 (91%)
NWMv2.1	Ref	136 (9.5%)
	Non-Ref	1302 (90%)
max(Model)	Ref	60 (7%)
	Non-Ref	850 (93%)

Table 6. The number (percent) of sites in each region for each hydrologic model application where the KGE score is less than the average day-of-year flow (AvgDOY) benchmark (underperforming sites); KGE = Kling–Gupta efficiency; NHMv1.0=National Hydrologic Model v1.0; NWMv2.1 = National Water Model v2.1; max(Model) = model with maximum KGE value from NHMv1.0 or NWMv2.1.

605

Model	West	Central	Southeast	Northeast
NHMv1.0	795 (55%)	412 (28%)	159 (11%)	91 (6%)
NWMv2.1	842 (59%)	370 (26%)	173 (12%)	54 (4%)
max(Model)	610 (67%)	213 (23%)	61 (7%)	27 (3%)

Figures
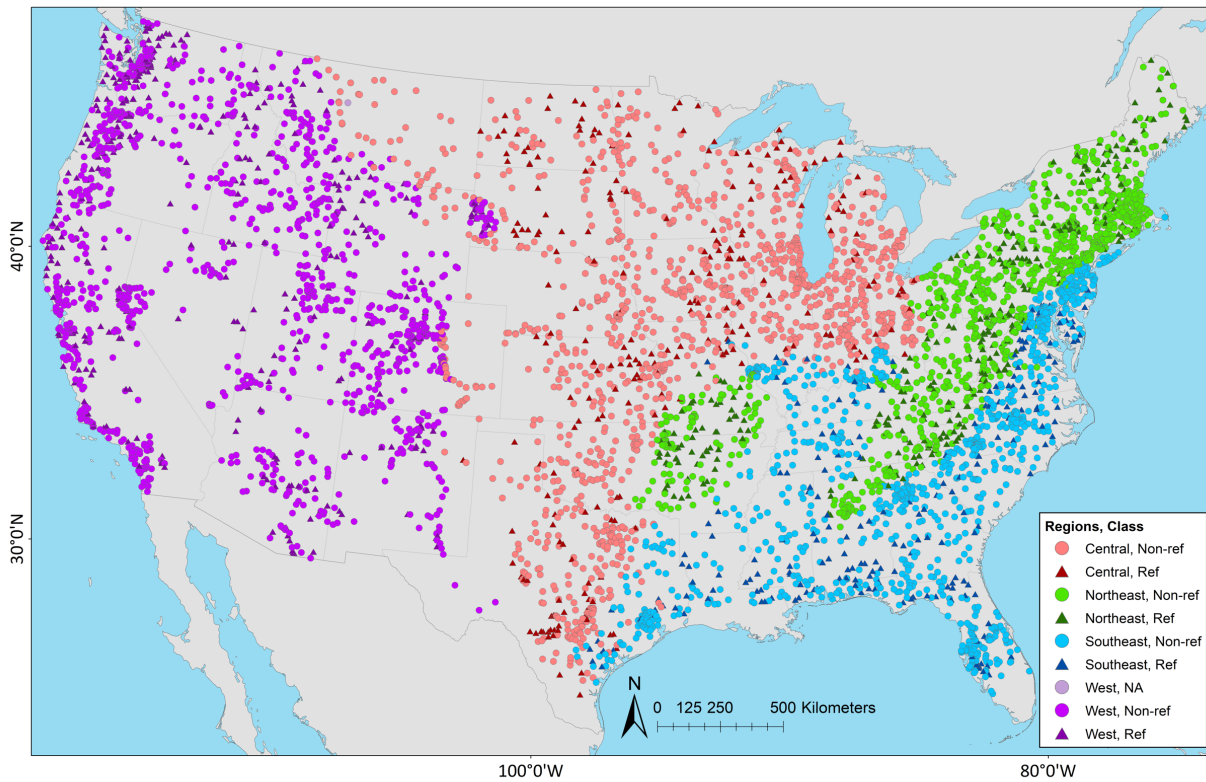
Figure 1: Site locations used in evaluation (n=5,390), including regions and classification. Regions were further combinations of aggregated ecoregions defined by Falcone (2010): Central (n=1,450) includes Central Plains, Western Plains, and Mixed Wood Shield; Northeast (n=1,218) includes Northeast and Eastern Highlands; Southeast (n=1,212) includes South East Plains and South East Coastal Plains; and West (n=1,510) includes Western Mountains and West Xeric. Classifications are from Falcone (2010): Reference (Ref, n= 1,115) and Non-Reference (Non-ref, n= 4,274); one gage was not designated (NA, n=1). Map Source: (Grannemann, 2010; Natural Earth Data, 2009; ESRI, 2022a; ESRI, 2022b).
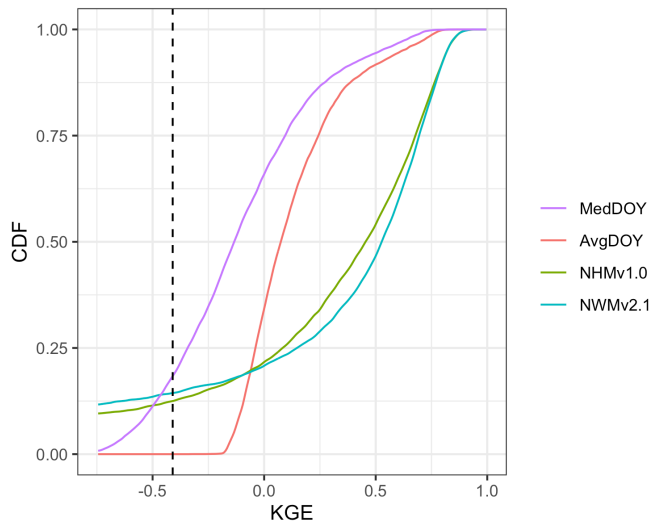
Figure 2: Cumulative density function (CDF) for Kling-Gupta efficiency (KGE) scores based on daily streamflow at U.S. Geological
Survey (USGS) gages for seasonal benchmarks based on the median day-of-year flows (MedDOY) and average day-of-year flows
(AvgDOY) and models: National Water Model v2.1 (NWMv2.1) and National Hydrologic Model v1.0 (NHMv1.0). Dotted vertical
line is KGE mean flow benchmark (=-0.41). For sites (n=1 for NWMv2.1 and n=16 for NHMv1.0) for which a KGE could not be
calculated (i.e., the modelled timeseries had all zero values for the entire timeseries), these are included as -Infinity in the CDFs.
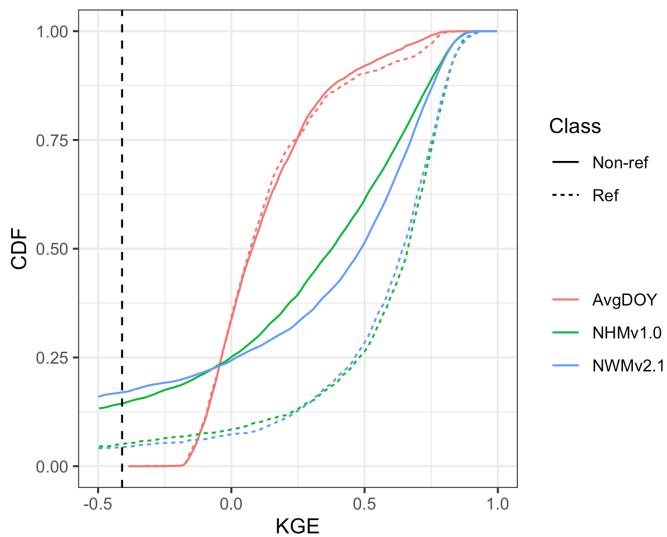
Figure 3: Cumulative density function (CDF) for Kling-Gupta efficiency (KGE) scores based on daily streamflow at U.S. Geological
Survey (USGS) gages for seasonal benchmark based on average day-of-year flows (AvgDOY) and models: National Water Model
v2.1 (NWMv2.1) and National Hydrologic Model v1.0 (NHMv1.0). Dotted vertical line is KGE mean flow benchmark (=-0.41).
Reference (Ref, n= 1,115) and Non-Reference (Non-ref, n= 4,274) classifications are from Falcone (2010).
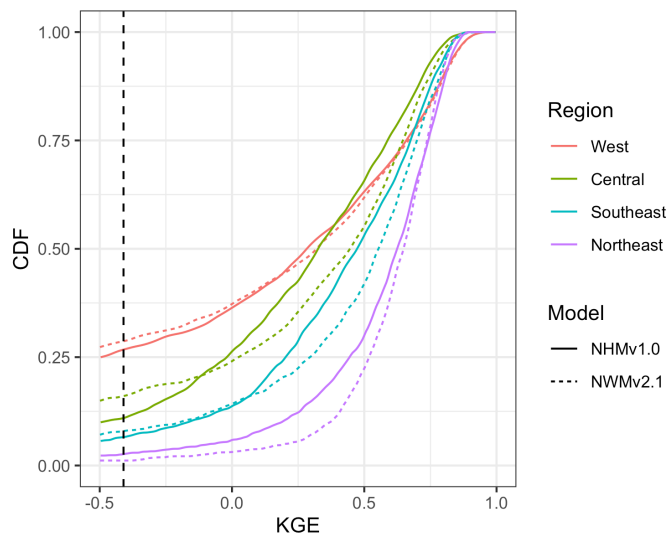
630 **Figure 4: Cumulative density function (CDF) for Kling-Gupta efficiency (KGE) scores based on daily streamflow at U.S. Geological Survey (USGS) gages for models: National Water Model v2.1 (NWMv2.1) and National Hydrologic Model v1.0 (NHMv1.0). Dotted vertical line is KGE mean flow benchmark (=-0.41). Regions are further combinations of aggregated ecoregions defined by Falcone (2010): Central (n=1,450) includes Central Plains, Western Plains, and Mixed Wood Shield; Northeast (n=1,218) includes Northeast and Eastern Highlands; Southeast (n=1,212) includes South East Plains and South East Coastal Plains; and West (n=1,510) includes**
635 **Western Mountains and West Xeric.**
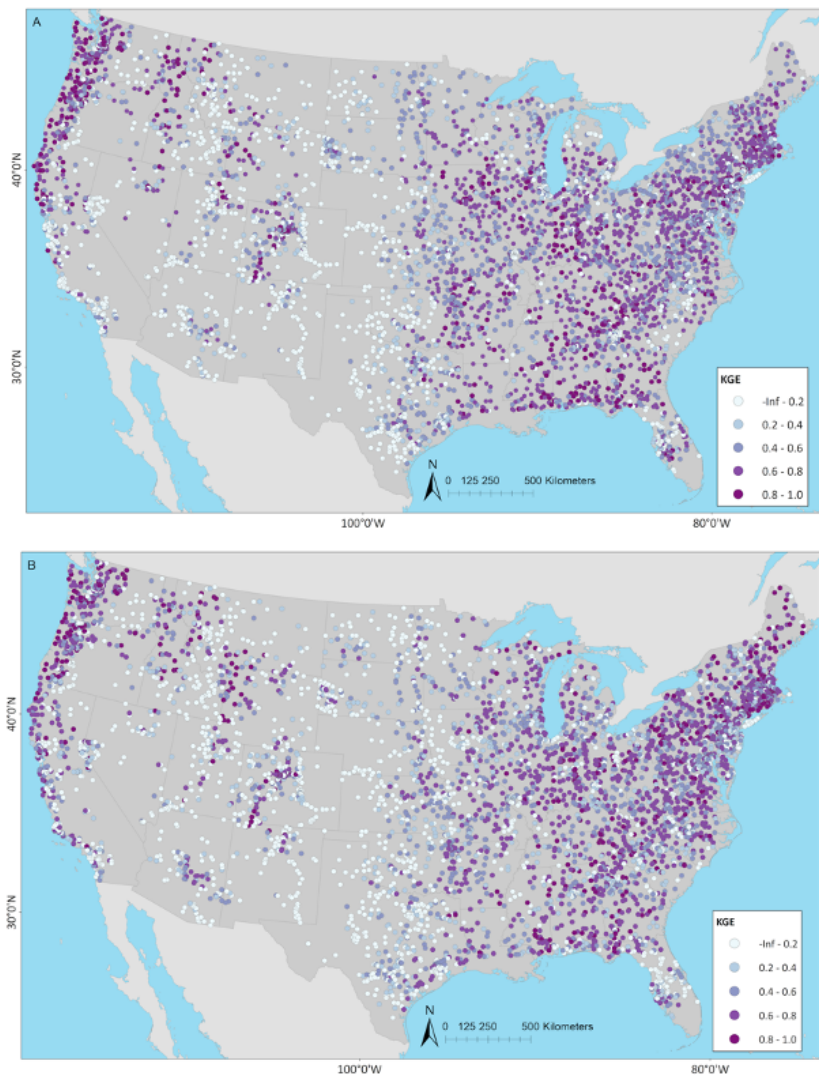
Figure 5: Kling–Gupta efficiency (KGE) based on daily streamflow at U.S. Geological Survey (USGS) gages for (A) National Water Model v2.1 (NWMv2.1) and (B) National Hydrologic Model v1.0 (NHMv1.0). Map Source: (Grannemann, 2010; Natural Earth Data, 2009; ESRI, 2022a; ESRI, 2022b).

640
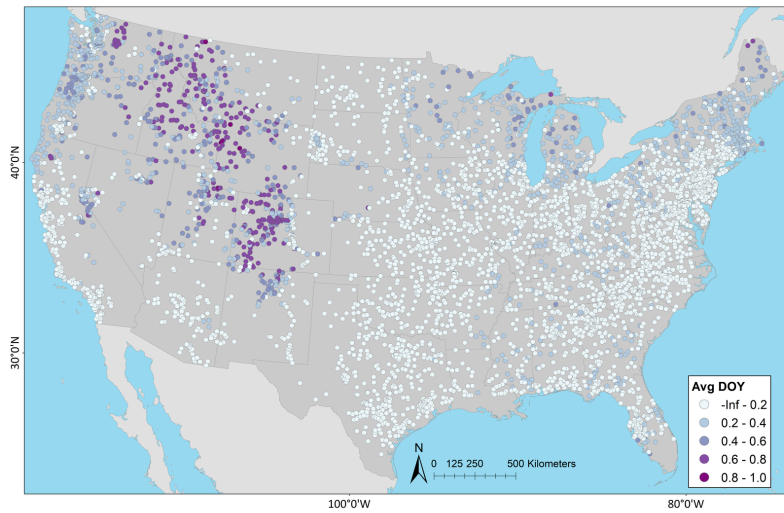
Figure 6: Kling–Gupta efficiency (KGE) based on daily streamflow at U.S. Geological Survey (USGS) gages using seasonal benchmark from average day-of-year flows (AvgDOY). Map Source: (Grannemann, 2010; Natural Earth Data, 2009; ESRI, 2022a; ESRI, 2022b).
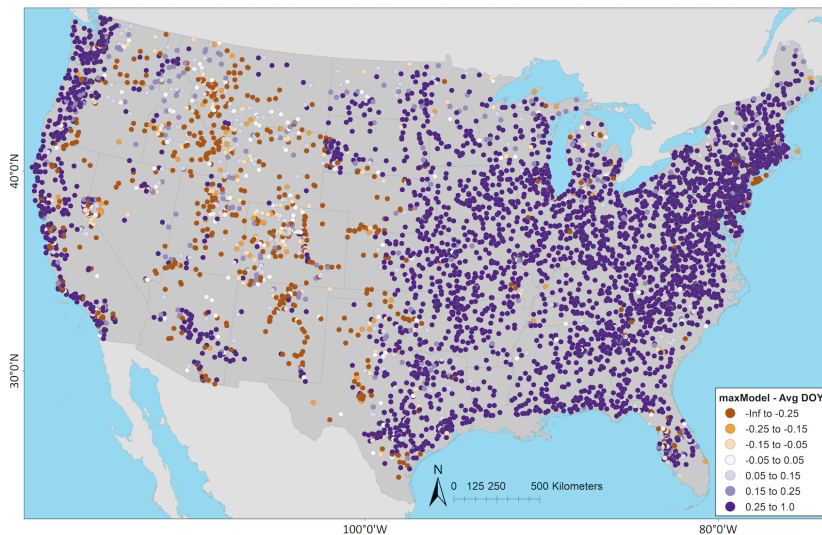
Figure 7: Difference between the Kling–Gupta efficiency (KGE) from the maximum model (maxModel) (i.e., the maximum KGE value from the National Water Model v2.1, NWMv2.1, or the National Hydrologic Model v1.0, NHMv1.0) minus the seasonal benchmark based on the average day-of-year flows (AvgDOY); negative (orange) indicates where AvgDOY has a higher (better) KGE, positive (purple) indicates that at least one of the models has a higher (better) KGE. Map Source: (Grannemann, 2010; Natural Earth Data, 2009; ESRI, 2022a; ESRI, 2022b).
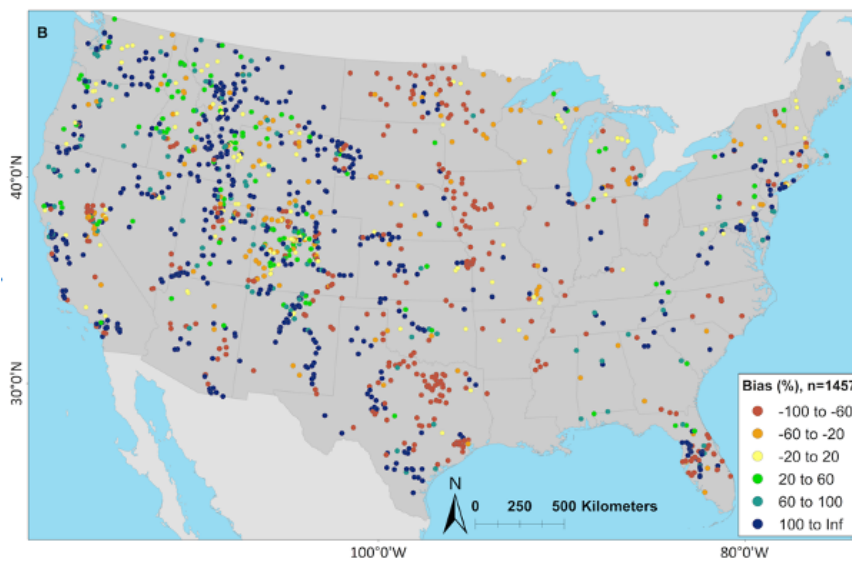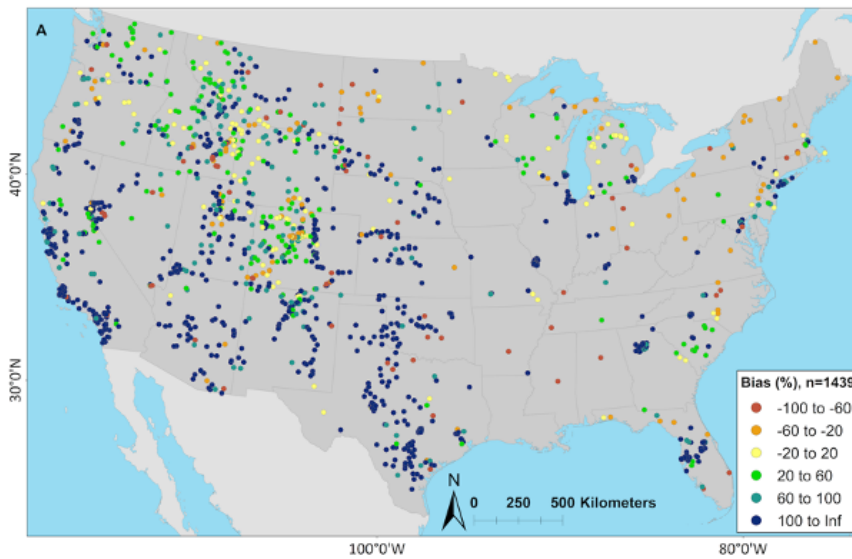
Figure 8: Percent bias (PBIAS) maps for National Water Model v2.1 (NWMv2.1) (A) and National Hydrologic Model v1.0 (NHMv1.0) (B), for sites where the KGE score is less than the average day-of-year flow (AvgDOY) benchmark. Cooler colors are where model application is overestimating volume and warmer colors are where model is underestimating volume. Map Source: (Grannemann, 2010; Natural Earth Data, 2009; ESRI, 2022a; ESRI, 2022b).

655
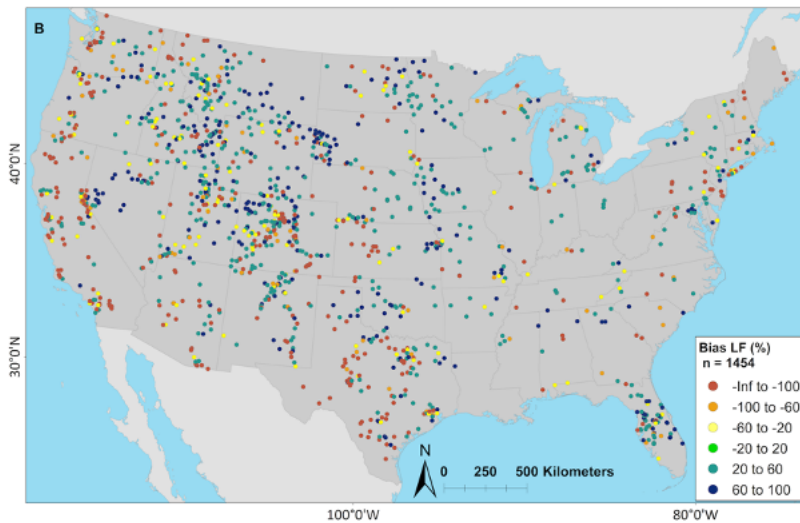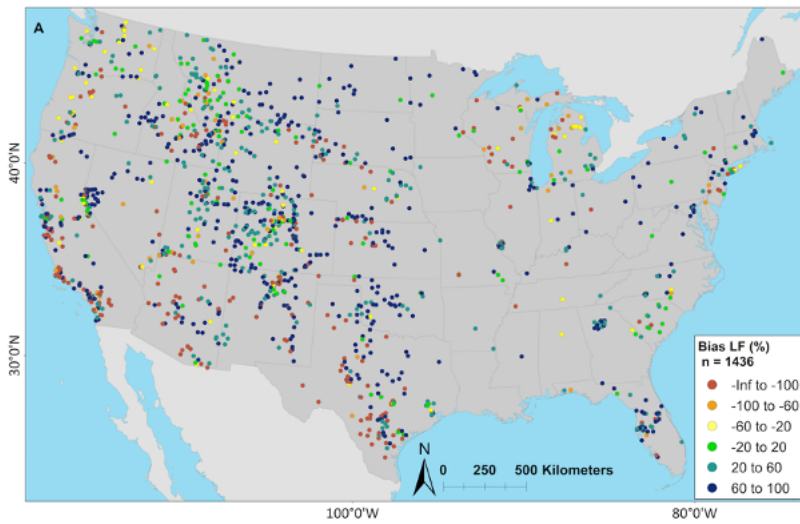
Figure 9: Percent bias low flow (PBIAS_LF, flows below 30% percentile) maps for National Water Model v2.1 (NWMv2.1) (A) and National Hydrologic Model v1.0 (NHMv1.0) (B), for sites where the KGE score is less than the average day-of-year flow (AvgDOY) benchmark. Cooler colors are where model application is overestimating low flows and warmer colors are where model is underestimating low flows. Map Source: (Grannemann, 2010; Natural Earth Data, 2009; ESRI, 2022a; ESRI, 2022b).